

Effect of Polyvinyl Alcohol (PVA)/Chitosan (CS) Weight Ratio on Morphology, Mechanical Properties, Antibacterial and Biodegradability of the Composite Film for Food Packaging Applications

Nur Aziah Suhada Naim¹, Muhammad Faiq Abdullah^{1,2,*}, Sung Ting Sam¹, Wan Ahmad Radi Wan Ahmad Yaakub¹

*faiq@unimap.edu.my

¹ Faculty of Chemical Engineering & Technology, Universiti Malaysia Perlis, Kompleks Pusat Pengajian Jejawi 3, 02600, Arau, Perlis, Malaysia

² Centre of Excellence Biomass Utilization, Universiti Malaysia Perlis, Kompleks Pusat Pengajian Jejawi 3, 02600, Arau, Perlis, Malaysia

Received: December 2024

Revised: May 2025

Accepted: June 2025

DOI: 10.22068/ijmse.3852

Abstract: Despite being an effective material for food packaging, chitosan (CS) exhibited poor ductility when processed into film, which restricted its use in this industry. In this study, composite films with enhanced properties were developed by incorporating polyvinyl alcohol (PVA) into CS through a simple solution casting method. The effects of different PVA/CS weight ratios (70:30, 50:50, and 30:70 w/w) on the morphology, mechanical properties, antibacterial activity, and soil degradation of the composite films were analyzed. Compared to the pristine PVA film, increasing the CS content in the PVA/CS composite film enhanced thickness, stiffness, roughness, antibacterial efficiency, and degradation rate, while reducing tensile strength and elongation at break. Fourier transform infrared (FTIR) spectroscopy revealed the highest intermolecular interactions in the PVA/CS composite film with 70:30 w/w. Antibacterial activity tests and soil burial analysis demonstrated that the PVA:70/CS:30 composite exhibited significantly higher antibacterial activity toward *Escherichia coli* and *Bacillus subtilis* bacteria compared to the PVA film, along with a moderate degradation rate of 76.76% following 30 days of soil burial, effectively balancing biodegradability and material integrity. These findings suggest that the PVA: 70/CS:30 composite is a promising alternative for sustainable and functional biodegradable packaging solutions.

Keywords: Chitosan, Polyvinyl alcohol, Composite film, Antibacterial, Packaging.

1. INTRODUCTION

The preservation of food safety and quality throughout the processing and consumption stages is greatly dependent on food packaging [1]. Commonly used materials for this purpose include paper, glass, metal, and plastic [2]. While plastics offer desirable properties for packaging, their long-lasting nature poses a significant environmental challenge in terms of pollution and waste accumulation [3]. The development of biodegradable alternatives presents a promising solution to this issue. One potential approach involves blending synthetic and natural polymers to create composite-based materials that offer enhanced mechanical properties and biodegradability as an adequate replacement for traditional plastic packaging.

Chitosan (CS), a natural polymer, has drawn significant interest in food, biomedical, and chemical manufacturing owing to its antibacterial, non-toxic, biodegradable, and biocompatible properties [4]. As such, coating and packaging

structures for food may benefit from CS due to its fascinating properties, for instance, its exceptional film formation capability and scent blockade characteristics while in the dry state [5]. In addition, CS exhibits significant antibacterial efficacy toward numerous pathogenic and spoilage microorganisms [6]. However, pure CS faces challenges such as insolubility in alkaline environments, reduced antibacterial effectiveness at higher pH levels (above 6.5), and poor mechanical properties. To resolve these problems, CS may be blended with synthetic polymers to improve its hydrophilicity, mechanical strength, and antibacterial properties while also improving its performance as a barrier against various chemicals [5, 7].

The fabrication of composite film is a practical approach to address the above problems. Composite films offer advantages over those made from their components due to their enhanced stability, biocompatibility, and mechanical strength. Polyvinyl alcohol (PVA) is among the synthetic polymers which has been extensively used as a packaging solution owing to its biodegradability, ease of

processing, high mechanical strength, availability, and excellent stability in acidic and alkaline environments [8]. PVA readily dissolves in hydrophilic polymers, including CS, as a result of hydrogen bonding between its hydroxyl groups and the amine and hydroxyl groups of CS [9]. PVA compatibility enables the immobilisation of CS through hydrogen bonding, thereby enhancing the mechanical properties of CS. However, excessive use of additives such as glycerol could result in the formation of a stiffer film with reduced tensile strength [10].

The distinctive functional properties of both polymers and their specific intermolecular interactions suggest that blending CS and PVA with an appropriate additive could enhance the resulting composites, potentially improving their mechanical characteristics [11]. Therefore, incorporating a plasticiser such as polyethylene glycol (PEG) into the polymers may be a practical approach to enhance the elasticity and mechanical strength of PVA/CS composites. The utilization of PEG as a plasticizer in PVA/CS composite films has not been extensively investigated before, highlighting the significance of this study. This work aims to produce PVA/CS composite film with different weight ratios for potential application in food packaging. It includes an analysis to assess how varying weight ratios impact the mechanical, biodegradable, antibacterial, and morphological properties, as well as other relevant attributes of the resulting PVA/CS composite films.

2. EXPERIMENTAL PROCEDURES

2.1. Materials

Partially hydrolyzed PVA powder ($\rho = 1.3 \text{ g/cm}^3$, $M_w = 16 \text{ KDa}$) and CS powder ($\rho = 1.08 \text{ g/cm}^3$, $M_w = 302.11 \text{ KDa}$) were acquired from Merck, USA and Sigma Aldrich, Malaysia, respectively. Glacial acetic acid and PEG powder were acquired from HmbG Chemical, Malaysia. Nutrient broth (casamino acids of 1 g/L; MgSO_4 of 15 g/L; NaCl of 5 g/L; tryptone of 10 g/L; yeast extract of 5 g/L), barium chloride and sulphuric acid were acquired from Sigma Aldrich, Malaysia. *Bacillus subtilis* (*B. subtilis*) and *Escherichia coli* (*E. coli*) were donated by the Biochemical Laboratory of the Faculty of Chemical Engineering & Technology at Universiti Malaysia Perlis (UniMAP), Malaysia.

2.2. Fabrication of PVA/CS Composite Film

The solutions of PVA and CS were separately prepared. For instance, 3 wt% of PVA solution was prepared by dissolving PVA powder in distilled water. The mixture was stirred continuously at 300 rpm and 80°C until it was fully dissolved. Next, 2 wt% of homogeneous CS solution was produced by dissolving CS powder in glacial acetic acid at 60°C . Subsequently, the freshly prepared CS solution was poured into a PVA solution at a predetermined PVA/CS weight ratio (70:30, 50:50, and 30:70 w/w) to yield a set of blend solutions, denoted as PVA:70/CS:30, PVA:50/CS:50, and PVA:30/CS:70, respectively. The blend solution was stirred at 600 rpm for at least 5 hours at 40°C . Per PVA/CS weight ratio, 1 wt% of PEG was added as plasticizer. The PVA/CS mixture was subsequently transferred onto a clean glass petri dish to form a composite film, and the poured solution was dried in a fume hood at room temperature for at least 48 hours. Pristine PVA and CS films were also prepared for comparison.

2.3. Morphological Analysis

An optical microscope (Motic BA200, Malaysia) was used to examine the morphology of the PVA/CS films, employing a 10X low-power objective magnification. Before microscopy viewing, the samples were cut into a square shape with dimensions of $30 \text{ mm} \times 30 \text{ mm}$. Meanwhile, a digital thickness gauge (Mitutoyo 547, Japan) was used to measure the film thickness at five different points with a precision of 0.01 mm. The average thickness was then calculated, along with its standard deviation (SD).

2.4. Surface Chemistry Analysis

The key functional groups in PVA and CS were examined using Fourier transform infrared (FTIR) spectroscopy (Perkin Elmer Spectrum 65) in single attenuated total reflectance (ATR) mode. Before analysis, the samples were cut into $10 \text{ mm} \times 10 \text{ mm}$ squares. Spectra were recorded over a wavelength range of 400 to 4000 cm^{-1} .

2.5. Tensile Testing

The tensile properties of the composite films were measured using a uniaxial tensile tester (Instron 5569, USA) by ASTM D882. Rectangular PVA/CS film samples ($60 \text{ mm} \times 7.5 \text{ mm}$) were prepared, and their weights were recorded before testing. Each sample was mounted onto the tensile

grips and stretched to failure at a crosshead speed of 1 mm/min, with a gauge length of 30 mm, under ambient conditions. For each PVA/CS composite film, five replicates were tested. The ultimate tensile strength (UTS), elongation at break (EB), and Young's modulus (YM) were calculated from the resulting stress-strain curves.

2.6. Antibacterial Activity

The antibacterial activity of the PVA/CS composite films was evaluated following the microbial dilution method described by Liu et al. [12] targeting *B. subtilis* and *E. coli*. To perform the test, a laminar airflow system and an autoclave were used to prevent contamination. The composite film was dissolved in distilled water at a ratio of 1:100 to produce the film's extract. The bacteria were then dissolved in 10 mL sterilized distilled water and visually compared with 0.5 McFarland turbidity standards. To prepare the inoculum, the bacterial solution was mixed with the nutrient broth at an optimal ratio of 1:100. For antibacterial testing, the extracted film and inoculum were combined in tubes at a 1:9 ratio. A control solution was prepared for both bacteria by mixing sterilized distilled water and inoculum using the same ratio. All test tubes were incubated at 37°C for 24 and 48 hours. The medium's turbidity was measured five times at 600 nm using a SpectraMax Plus 384 spectrophotometer. After each incubation period, the antibacterial activity was determined using Eq. (1):

$$\text{Antibacterial activity (\%)} = 1 - \frac{\text{OD}_2}{\text{OD}_1} \times 100\% \quad (1)$$

where OD_1 represents the optical density of the bacteria in the medium, while OD_2 corresponds to the optical density of the bacteria in the solution in contact with the PVA/CS films.

2.7. Soil burial Test

The PVA/CS composite films were shaped into 30 mm × 30 mm squares and buried for 30 days. The soil burial testing was performed at Tan Sri Aishah Ghani Residential College, Perlis, Malaysia, at coordinates 6°27'14.9508", 100°9'25.9492". The temperature of the soil was monitored periodically using a soil survey instrument (Giant Force, Taiwan). The samples were buried 10 cm deep in the ground. The degradation of the samples was measured every 6 days. At a pre-determined time point, the sample was removed from the soil and cleaned carefully with tissue paper. Excess soil on the film surface was gently cleaned before weight

measurement was performed. The film's weight loss was determined by Eq. (2):

$$\text{Weight loss (\%)} = \frac{W_i - W_d}{W_i} \times 100\% \quad (2)$$

where W_i is the film's initial weight and W_d is the weight of the film after it has been removed from the soil.

2.8. Statistical Analysis

The statistical analysis was performed using one-way analysis of variance (ANOVA) with Minitab software, with a significance level of $p < 0.05$. All experiments were conducted in triplicate, and the data are presented as the mean ± standard deviation (SD).

3. RESULTS AND DISCUSSION

3.1. Morphological Analysis

The morphology of the as-produced films was analysed using optical microscopy to investigate how variations in PVA/CS weight ratios affected their surface characteristics. Fig. 1 shows the morphology of the PVA/CS cast-composite films in comparison to the pristine PVA and CS films. It has been revealed that the composite films developed a rough surface and coarse structure with white areas when the concentration of CS was increased, consistent with the findings by [13]. However, all PVA/CS composite films, regardless of the weight ratio, exhibited an uneven surface, air bubbles, and pores, indicating inadequate polymer mixing and inconsistent CS dispersion in the PVA/CS matrix. Since PEG is a highly hydrophilic polymer and its incorporation into PVA/CS film was not considered in previous studies, this explanation seems plausible. Wang et al. [14] demonstrated that increasing the water content in a PEG film led to increased surface roughness due to hydrogen bonding between the hydroxyl groups of PEG and water molecules. These hydrogen bonds can disrupt the film's organisation and structure, resulting in a rougher surface [14]. Furthermore, it has been postulated that an acetic acid solution with a concentration below 90%, due to the water content in the PVA solution, may result in micelle formation [15]. This phenomenon can interfere with the uniform dispersion of CS on the surface of PVA/CS films. From Fig. 1, it was evident that the surface of the pristine PVA film contains irregularities such as uneven surfaces, roughness, air bubbles, pores, cracks, or droplets. This finding significantly

contrasts with a previous study by Al-Tayyar et al. [16], which reported that pure PVA film had good structural integrity without surface irregularities. Pristine CS film, on the other hand, had a smoother and more consistent surface, free of imperfections. This difference can be attributed to the deprotonation of CS, which enhances its film-forming ability as detected by FTIR spectroscopy, resulting in improved smoothness of the CS film [17]. Deprotonation causes the amino groups within CS molecules to lose protons and acquire negative charges, leading to repulsion between molecules that prevents clumping and yields a smooth, even film. Additionally, the preparation of pristine CS film without water molecules is speculated to contribute to its smoother appearance compared to PVA and PVA/CS films.

The microscopic images revealed the varying morphologies of the films. The pure PVA film exhibited good structural integrity; however, its smoothness was compromised by air bubbles, indicating rapid evaporation of the PVA solvent during the casting process. Adding CS to the PVA matrix resulted in decreased smoothness and the appearance of visible black patches [9]. At low CS concentrations, the surface remained relatively smooth with only a few black spots. However, when CS content exceeded 70%, these black spots became predominant. This observation can be attributed to the inconsistent dispersion of CS in the PVA/CS matrix, as evidenced by digital images of the film's condition.

In the food packaging industry, selecting a suitable film depends significantly on its thickness. Table 1 presents the average film thickness of the PVA/CS composite, as well as that of pristine PVA and CS films, measured at five different locations. The use of a consistent volume (15 mL) of casting solution in this study led to variations in film thickness.

Table 1. Average film thickness of PVA/CS composite, pristine PVA, and pristine CS film prepared in this study

Sample	Thickness (mm)
PVA:100	$0.056 \pm 0.002^{**}$
PVA:70/CS:30	$0.092 \pm 0.002^{**}$
PVA:50/CS:50	$0.100 \pm 0.002^{**}$
PVA:30/CS:70	$0.110 \pm 0.001^{***}$
CS:100	$0.069 \pm 0.001^{***}$

The data are presented as mean \pm SD with $n=3$. Distinct symbols indicate significant differences: * for $p<0.05$, ** for $p<0.01$ and *** for $p<0.001$.

The average thickness of pure PVA and CS film was 0.056 mm and 0.069 mm, respectively, while the thickness of PVA/CS films ranged from 0.092 to 0.110 mm. A significant variation ($p<0.05$) in the film's thickness was observed, suggesting an uneven distribution within the film matrix. The increase in thickness of PVA/CS films can be attributed to the addition of CS. It has been postulated that a higher content of CS leads to increased thickness due to wider hydration layers formed by positively charged groups from CS chains [18]. The high prevalence of -OH and -NH₂ groups in the CS molecule promotes stronger intermolecular and intramolecular hydrogen bonding. This enhanced bonding capacity leads

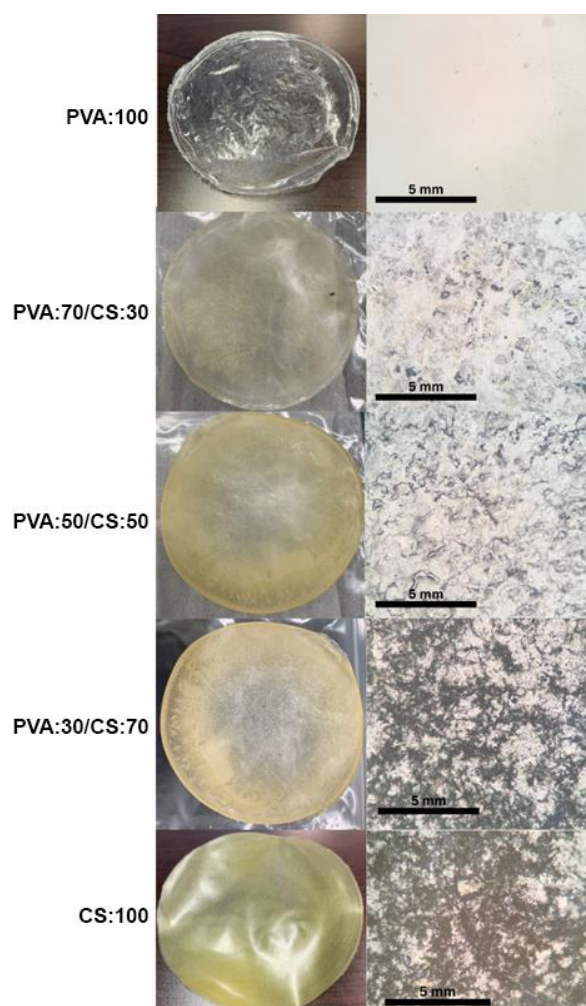


Fig. 1. Comparative images of a PVA/CS composite film prepared at varying weight ratios, including digital (left) and optical microscopy views (right) at 10X magnification

to improved water retention, resulting in the formation of thicker films [19].

Contrary to expectations, the pure CS film was thinner than the PVA/CS film. This difference may be attributed to a higher concentration of glacial acetic acid in the pure CS film, which has a faster evaporation rate compared to when it is in the PVA/CS film. Gavriel et al. [20] suggested that glacial acetic acid evaporates more rapidly than water due to its weaker hydrogen bond. In contrast, the fabrication of PVA/CS involves distilled water, indicating stronger hydrogen bond formation. As a result, when the CS solution is applied to a surface, the rapid evaporation of glacial acetic acid results in a thinner film compared to the PVA/CS composite films.

Commercial food packaging films exhibit varying thicknesses due to factors such as the specific food product, desired barrier properties, and the packaging method employed [21]. They can range from thin layers, around 0.010-0.025 mm, to thicker films of several hundred micrometres. Flexible food packaging films typically have a thickness between 0.030-0.080 mm, but may vary depending on material and product needs [22]. Thinner films are used for snack bags, while thicker materials are needed for frozen food packaging to provide added protection against

freezer burn and mechanical damage. The PVA/CS composite film falls within this standard range, with a thickness of 0.092 to 0.11 mm, making it suitable for commercial industry applications as it is similar in thickness to available food packaging film options.

3.2. FTIR Analysis

FTIR spectroscopy is a valuable method for recognizing distinctive molecular vibrations that can help determine the structure and composition of materials, as well as the chemical bonds within a specific sample. Fig. 2 portrays the FTIR spectra of pristine PVA, pristine CS, and PVA/CS composite films produced in this study.

The FTIR spectral analysis reveals that the non-bonded hydroxyl group typically exhibits a band in the range of 3450 to 3600 cm^{-1} , while the hydrogen-bonded hydroxyl group is observed within 3200-3500 cm^{-1} , consistent with the findings reported by Wardhono et al. [23]. For PVA, the broad peak at approximately 3344 cm^{-1} corresponds to the stretching vibration of the O-H bond, and the peak at 1466 cm^{-1} is attributed to the bending vibration of the hydroxyl group. The vibration band at 1098 cm^{-1} can be credited to the C-O stretching of the acetyl groups present on the PVA backbone [24].



Fig. 2. FTIR spectra of PVA/CS composite films and pristine PVA and CS films

Additionally, the peak observed at 1665 cm^{-1} is attributed to the C=O stretching vibration in the acetyl group, while the peak at 2889 cm^{-1} arises from the asymmetric stretching vibration of the C–H bond in the methylene group [23].

The FTIR spectrum of CS exhibited characteristic peaks at 2886 , 2995 , 2889 , 1641 , and 1541 cm^{-1} , which were attributed to the stretching vibrations of hydroxyl and amino groups, symmetric C–H bonds, C=O stretching, and asymmetric stretching of amino bonds, respectively. Additionally, the peaks observed at 963 and 1223 cm^{-1} were primarily associated with the saccharide moiety, while the peak at 1250 cm^{-1} was linked to the amino group of CS. Furthermore, the bands detected at 1072 and 1020 cm^{-1} were attributed to C=O stretching [23].

The FTIR spectra of the PVA/CS composite films, with varying PVA and CS compositions, showed distinct changes. As the CS content increased, there was a clear rise in the band intensity around 3314 cm^{-1} , 3344 cm^{-1} , and 3367 cm^{-1} . These bands were attributed to the hydroxyl group stretching vibrations of PVA and the secondary amide group of CS [9], indicating a hydrogen bonding interaction between the two polymers. Moreover, the characteristic shape of the CS spectrum was altered, and the peaks shifted to a lower frequency range when PVA and CS were blended. This shift was attributed to the formation of hydrogen bonds between the hydroxyl groups of PVA and the hydroxyl or amine groups of CS. Interestingly, the amino group peak at 1250 cm^{-1} disappeared from

the CS spectra, and the presence of the secondary amine N–H and the O–H group was indicated by the band at 1077 cm^{-1} [23]. The characteristic bands of the PVA/CS blend film resembled those of PVA, and the strong amorphous C=O stretching vibrations of PVA remained constant across all films. The spectrum of the PVA/CS blend film also showed that the peaks related to the C=O of PVA shifted to a higher wavenumber, and the intensity of some peaks in pure CS and PVA decreased, suggesting intermolecular interactions between CS and PVA molecules in the composite films [13].

3.3. Tensile Analysis

Fig. 3 illustrates the typical stress-strain behavior of the as-produced PVA/CS composite, pristine PVA, and pristine CS films, while their respective UTS, EB, and YM values are presented in Fig. 4. The tensile test results revealed that increasing the CS content in the PVA/CS composite film led to a decline in tensile strength and maximum elongation, but an enhancement in film stiffness. This finding aligns with the study by Fakraoui and co-workers [25], which demonstrated that the UTS and EB of PVA/CS blend films decrease with an increase in CS percentage. The UTS of pristine PVA and CS films were determined to be $20.73 \pm 0.71\text{ MPa}$ and $16.27 \pm 0.68\text{ MPa}$, respectively, while their respective EB were $52.14 \pm 0.41\%$ and $1.75 \pm 0.05\%$. The results suggest that the presence of PVA may significantly influence the tensile strength and maximum deformation capacity of the composite films [9].

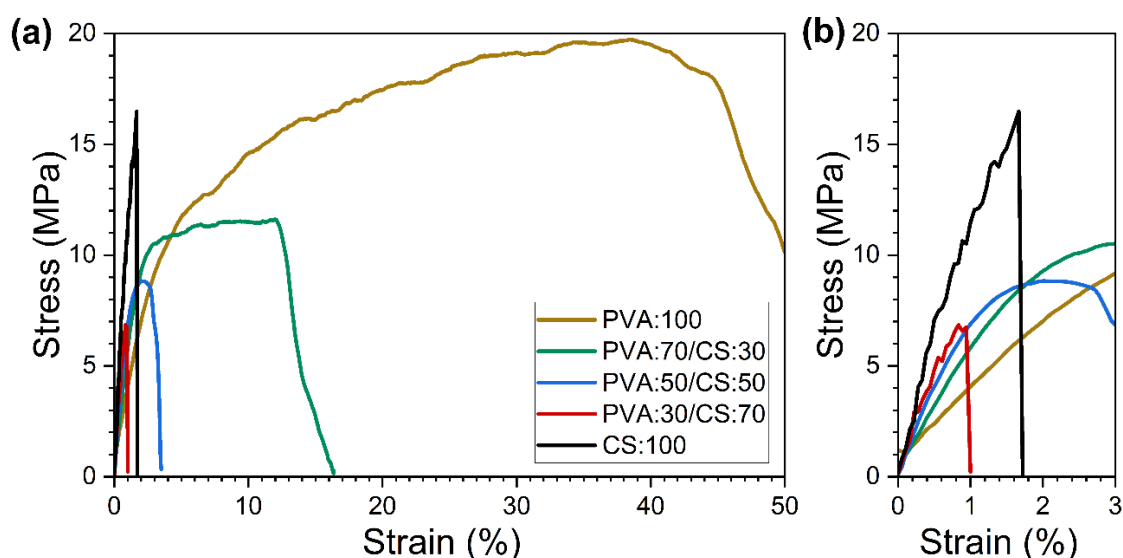


Fig. 3. Typical stress-strain curve for a) the as-prepared PVA/CS composite, pristine PVA and CS films, and b) enlarged plot of the stress-strain curve at 0-3% strain region



Fig. 4. The tensile properties, including a) UTS, b) EB, and c) YM of the PVA/CS composite films were compared to those of pristine PVA and CS films. Distinct symbols indicate significant differences: * for $p < 0.05$, ** for $p < 0.01$ and *** for $p < 0.001$

As the presence of CS increased and the content of PVA decreased in the blend films, the flexibility of the PVA/CS composites significantly diminished. Tensile strength and ductility tended to decline as the CS content increased. For example, the UTS of the PVA/CS composite film decreased from 12.80 ± 0.95 MPa to 6.83 ± 0.55 MPa when the CS weight percentage increased from 30% to 70%. Similar trends were observed for the EB, which decreased substantially from $16.26 \pm 0.31\%$ to $1.11 \pm 0.12\%$ with the same increase in CS weight percentage. Although pure CS exhibits higher UTS than all PVA/CS composite samples, its EB was significantly lower than that of the PVA:70/CS:30 sample. This suggests that incorporating a higher CS weight ratio may result in a film with brittle characteristics, which may be

unsuitable for packaging applications.

The YM values of the PVA/CS composite films exhibited a contradictory trend. As the CS weight percentage increased from 30% to 70%, the YM of the PVA/CS composites increased from 354.43 ± 0.95 MPa to 972.50 ± 0.70 MPa. In contrast, pristine PVA and CS films exhibited YM values of 324.20 ± 0.46 MPa and 1347.90 ± 0.80 MPa, respectively. This divergent behavior can be attributed to the distinctive roles played by CS within the composite matrix. Such contradictory observations are not uncommon in polymer composites, where the individual components contribute differently to the overall mechanical properties [26]. The enhanced stiffness of PVA/CS composite films with higher CS content was postulated to be due to the formation of strong hydrogen bonds between the amino and hydroxyl groups of CS and the hydroxyl groups of PVA, creating a tightly integrated polymer matrix that improves the film's rigidity [17]. Additionally, at higher CS weight ratios, phase separation may occur, leading to the formation of CS-rich domains within the PVA matrix. These rigid CS-rich domains act as fillers that impede the flexibility of the surrounding PVA chains, further increasing the film's stiffness but simultaneously reducing its ductility and ability to withstand high levels of stress before failure.

The observed incompatibility between CS and PVA, as seen in the film morphology despite the addition of a plasticizer, may have influenced the mechanical properties of the PVA/CS composite films. This is evidenced by the lower UTS of all PVA/CS composites compared to both pristine PVA and pristine CS films. This phenomenon can be attributed to the effect of non-solvents, where water is a non-solvent for CS, while glacial acetic acid is a non-solvent for PVA. Despite the incompatibility between CS and PVA and the resulting lower UTS of all PVA/CS composites compared to pure PVA and CS films, the PVA:70/CS:30 composite exhibited tensile properties that were not significantly different from the pure PVA film. This is a crucial finding, as it maintains a balance between mechanical performance and other beneficial properties, such as soil degradation and antibacterial activity. Additionally, the presence of CS in the PVA:70/CS:30 composite imparts enhanced antibacterial activity, which will be discussed in the subsequent section. This added functionality

makes the PVA:70/CS:30 composite an excellent alternative for food packaging films, combining adequate mechanical properties, effective degradation rate, and improved antibacterial properties due to the inclusion of CS.

3.4. Antibacterial Activity

The study presented in Fig. 5 examined the antibacterial activity of PVA/CS composite films and pure PVA and CS films against *E. coli* and *B. subtilis*. After 48 hours, the antibacterial efficacy against *B. subtilis* was $16.07 \pm 0.02\%$, $30.00 \pm 0.02\%$, $39.48 \pm 0.03\%$, and $46.48 \pm 0.02\%$ for CS concentrations of 30%, 50%, 70%, and 100%, respectively. For *E. coli*, the antibacterial activity was $13.51 \pm 0.01\%$, $26.80 \pm 0.08\%$, $35.22 \pm 0.05\%$, and $44.67 \pm 0.02\%$ for the corresponding CS concentrations. These findings demonstrate that all the tested films were more effective in inhibiting the growth of the Gram-positive bacterium *B. subtilis* than the Gram-negative *E. coli* after 48 hours.

The results indicate that Gram-positive bacteria are more susceptible to inhibition by the films. These findings align with those of previous studies [16, 27]. This disparity may be attributed to the structural differences in the cell walls of Gram-positive and Gram-negative bacteria. Gram-positive bacteria, such as *B. subtilis*, possess a thick, porous peptidoglycan layer that constitutes their cell wall. This allows CS to penetrate the cell and disrupt its metabolic processes easily [12]. In contrast, the outer membrane of Gram-negative bacteria, such as *E. coli*, is composed of phospholipids and lipopolysaccharides, and its peptidoglycan layer is thinner and more permeable to ions. Due to its barrier function, this outer membrane reduces the antibacterial effectiveness of CS by impeding its entry into the cell [28].

Meanwhile, the pristine PVA film exhibited antibacterial activity of only $5.58 \pm 0.01\%$ against *E. coli* and $5.33 \pm 0.01\%$ against *B. subtilis* after 48 hours of cultivation. The pristine PVA film exhibited a negligible antibacterial effect on both *E. coli* and *B. subtilis*, suggesting that PVA, on its own, does not substantially impede bacterial proliferation or propagation. This is based on the results reported by Bakhsheshi-Rad et al. [29]. In contrast, the PVA/CS composite films exhibited markedly greater antibacterial efficacy compared to pure PVA films. This enhanced antibacterial activity can be ascribed to the intrinsic properties

of CS. As the concentration of CS in the films increased, the antibacterial activity also increased proportionally. This is because the higher availability of free amino groups in CS provides more positive charges. These positive charges interact with the negatively charged components of bacterial cells, thereby disrupting DNA replication and protein synthesis, ultimately resulting in the observed antibacterial effect [12].

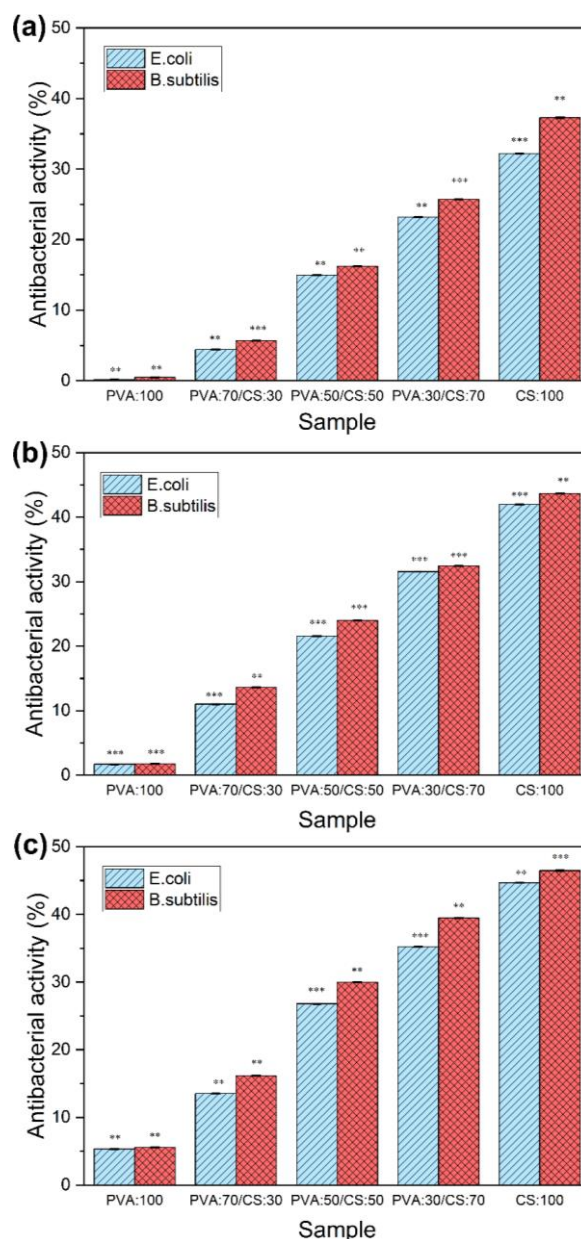


Fig. 5. Antibacterial activity of PVA/CS composite, and pristine PVA and CS film against *E. coli* and *B. subtilis* at a) 0 hour, b) 24 hours, and c) 48 hours cultivation. The data are presented as mean \pm SD with $n=3$. Distinct symbols indicate significant differences: * for $p < 0.05$, ** for $p < 0.01$ and *** for $p < 0.001$

3.5. Soil Burial Analysis

Several factors, including polymer structure, chain length, soil conditions, film thickness, and the presence of microorganisms in the soil influence the biodegradation rate of polymeric materials [30]. Fig. 6 and Fig. 7 illustrate the biodegradation of films through changes in surface appearance and weight loss over 30 days, respectively. After 30 days, all tested films exhibited shrinkage, increased brittleness, and a wrinkled appearance, with the pure CS film showing the most severe deterioration. Notably, the higher the CS content in the PVA matrix, the greater the degradation observed. PVA films, however, displayed minimal changes after 30 days, as PVA biodegradation requires specific conditions and microorganisms not commonly found in natural environments [31].

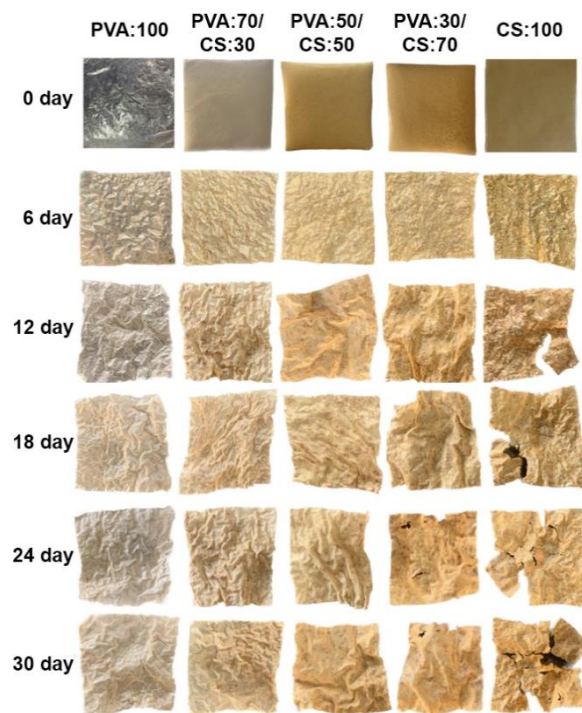


Fig. 6. Comparative digital images of surface morphology of PVA/CS composite films against pristine PVA and CS films following 30 days of soil burial

For PVA/CS films, noticeable surface deterioration appeared after 12 days of soil burial. Small holes on the film surface indicated degradation, and by the end of the test, the films had begun to disintegrate. The presence of CS likely enhanced microbial degradation more effectively than in pure PVA films [31]. Films with higher CS content aggregated more soil on their surfaces,

correlating with their higher hydrophilicity due to hydroxyl and amino groups in the CS structure [12]. This suggests a link between a film's hydrophilicity and its biodegradation rate.

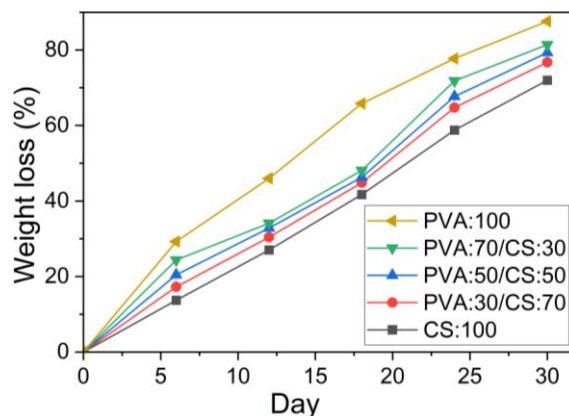


Fig. 7. Comparative analysis of weight loss between PVA/CS composite films and pristine PVA and CS films following 30 days of soil burial

Fig. 6 shows that the morphological changes were consistent with the weight loss rates for all films (Fig. 7). The prepared films exhibited a weight loss of about 71-88%, indicating active biodegradation by soil microorganisms and moisture. During the first 6 days, PVA/CS films lost 17-25% of their weight, increasing to 44-49% by 18 days. After 30 days, 76-82% of the PVA/CS blends had degraded, comparable to previous reports on PVA/CS composites [29, 32]. Pristine PVA film degraded more slowly (72%) compared to the PVA/CS composites after 30 days, consistent with findings by Ahmed et al. [33]. PVA, although biodegradable and susceptible to hydrolysis, shows higher resistance to soil burial degradation. The degradation of CS blends in soil is influenced by water absorption and the susceptibility of components to microbial or enzymatic attack [34]. CS, being naturally derived, is biodegradable and susceptible to microbial attack, resulting in higher degradation percentages for blend films compared to pure PVA films [4]. The soil environment contains diverse microorganisms, including thermophilic, psychrophilic, and mesophilic types, which adjust their biological activity in response to temperature changes. The heterogeneity of soil and its microbial inhabitants makes it challenging to obtain uniform samples and accurately describe ecological relationships. Chitosanases are enzymes that accelerate the hydrolytic breakdown of CS. Numerous species of chitosanase microorganisms,

such as *Bacillus*, *Arthrobacter*, *Penicillium*, *Aspergillus*, and *Streptomyces* are prevalent in soil, and they have been identified as efficient degraders of CS [35]. Although CS possesses antimicrobial properties that inhibit the growth of harmful microorganisms, it can still be effectively broken down by specific microbes like *Streptomyces* that thrive in the soil environment. Among the studied blend ratios, PVA:70/CS:30 stands out as the most suitable composition for the composite film due to its optimal balance between mechanical properties and biodegradability. The PVA:70/CS:30 blend exhibits superior tensile properties, including higher tensile strength and ductility, which are essential for ensuring the durability and performance of packaging films. Additionally, the PVA:70/CS:30 blend demonstrates a more controlled degradation rate, with a weight loss of 76.76% over 30 days. This is slower compared to the higher degradation rates observed in PVA:50/CS:50 and PVA:30/CS:70 blends, which show weight losses of 79.31% and 81.42%, respectively. The moderate degradation rate of the PVA:70/CS:30 composite ensures that the film maintains its structural integrity for a more extended period, making it a more practical and effective packaging material. By combining good tensile properties with a not-too-rapid degradation rate, the PVA:70/CS:30 blend provides a balanced solution that enhances the film's functionality and longevity in practical applications.

4. CONCLUSIONS

This study investigated the effects of varying PVA/CS weight ratios on the morphological, mechanical, antibacterial, and biodegradable properties of composite films for potential food packaging applications. Morphological analysis revealed that increasing the CS content resulted in a coarse and rough surface with white patches, air bubbles, and pores, indicating inadequate polymer mixing and inconsistent CS dispersion. Despite these challenges, the PVA:70/CS:30 composite exhibited tensile properties comparable to those of pure PVA, striking a balance between mechanical performance and other advantageous properties. Tensile analysis demonstrated that a higher CS content reduced the tensile strength and ductility of PVA/CS composite films, but enhanced the film stiffness. The PVA:70/CS:30 composite exhibited a favorable balance with good UTS and

EB, making it suitable for durable and flexible food packaging.

Antibacterial evaluations revealed that all PVA/CS composites exhibited substantially higher antibacterial efficacy compared to pure PVA film, with the PVA:70/CS:30 composite demonstrating enhanced antibacterial properties against both *E. coli* and *B. subtilis*. This amplified antibacterial activity can be attributed to the presence of CS, which disrupts bacterial cell walls and impedes bacterial growth. Soil burial analysis further corroborated the suitability of the PVA:70/CS:30 composite, as its moderate degradation rate of 76.76% over 30 days ensured the film maintained structural integrity during use, providing a practical and effective solution for packaging applications. The presence of specific soil microorganisms effectively degraded the CS component, while the PVA matrix exhibited resistance to rapid degradation, ensuring extended functional lifespan. In conclusion, the PVA:70/CS:30 composite film proves to be the most suitable weight ratio for food packaging applications. This can be attributed to its well-balanced mechanical attributes, efficient biodegradation profile, and improved antibacterial performance. These desirable properties position it as a promising alternative to conventional packaging materials, enabling both sustainability and enhanced functionality. The insights gleaned from this study offer valuable inputs for the development of advanced biodegradable packaging films, thereby contributing to the mitigation of plastic waste and the advancement of eco-friendly packaging solutions.

5. ACKNOWLEDGEMENT

This work was supported financially by the Faculty of Chemical Engineering & Technology, Universiti Malaysia Perlis (UniMAP), Malaysia.

REFERENCES

- [1] Díaz-Montes, E., "Polysaccharide-Based Biodegradable Films: An Alternative in Food Packaging". *Polysacch.*, 2022, 3, 761-775.
- [2] Yadav, M. and Chiu, F.-C., "Cellulose nanocrystals reinforced κ -carrageenan based UV resistant transparent bionanocomposite films for sustainable packaging applications". *Carbohydr. Polym.*, 2019, 211, 181-194.

- [3] Navasingh, R. J., Gurunathan, M. K., Nikolova, M. P., and Królczyk, J. B., "Sustainable Bioplastics for Food Packaging Produced from Renewable Natural Sources". *Polymers*, 2023, 15, 3760.
- [4] Jiang, A., Patel, R., Padhan, B., Palimkar, S., Galgali, P., Adhikari, A., Varga, I., and Patel, M., "Chitosan Based Biodegradable Composite for Antibacterial Food Packaging Application". *Polymers*, 2023, 15, 2235.
- [5] Barik, M., BhagyaRaj, G. V. S., Dash, K. K., and Shams, R., "A thorough evaluation of chitosan-based packaging film and coating for food product shelf-life extension". *J. Agric. Food Res.*, 2024, 16, 101164.
- [6] Måsson, M., "The quantitative molecular weight-antimicrobial activity relationship for chitosan polymers, oligomers, and derivatives". *Carbohydr. Polym.*, 2024, 337, 122159.
- [7] Jiao, X., Xie, J., Hao, M., Li, Y., Wang, C., Zhu, Z., and Wen, Y., "Chitosan Biguanidine/PVP Antibacterial Coatings for Perishable Fruits". *Polymers*, 2022, 14, 2704.
- [8] Zhang, W., Khan, A., Ezati, P., Priyadarshi, R., Sani, M. A., Rathod, N. B., Goksen, G., and Rhim, J.-W., "Advances in sustainable food packaging applications of chitosan/polyvinyl alcohol blend films". *Food Chem.*, 2024, 443, 138506.
- [9] Vlad-Bubulac, T., Hamciuc, C., Rîmbu, C. M., Aflori, M., Butnaru, M., Enache, A. A., and Serbezeanu, D., "Fabrication of Poly(vinyl alcohol)/Chitosan Composite Films Strengthened with Titanium Dioxide and Polyphosphonate Additives for Packaging Applications". *Gels*, 2022, 8, 474.
- [10] Paudel, S., Regmi, S., and Janaswamy, S., "Effect of glycerol and sorbitol on cellulose-based biodegradable films". *Food Packag. Shelf Life*, 2023, 37, 101090.
- [11] Vehapi, M., Yilmaz, A., and Özçimen, D., "Fabrication of Oregano-Olive Oil Loaded PVA/Chitosan Nanoparticles via Electrospraying Method". *J. Nat. Fibers*, 2021, 18, 1359-1373.
- [12] Liu, F., Zhang, X., Xiao, X., Duan, Q., Bai, H., Cao, Y., Zhang, Y., Alee, M., and Yu, L., "Improved hydrophobicity, antibacterial and mechanical properties of polyvinyl alcohol/quaternary chitosan composite films for antibacterial packaging". *Carbohydr. Polym.*, 2023, 312, 120755.
- [13] Turanli, A., Altinkok, C., Kacakgil, E. C., Dizman, C., and Acik, G., "A comprehensive study on the comparison between casted films and electrospun nanofibers of poly (vinyl alcohol)/chitosan blends: wettability, thermal, antioxidant, and adsorbent properties". *Int. J. Biol. Macromol.*, 2025, 315, 144467.
- [14] Wang, X., Zhao, Y., and Wen, X., "Effect of Polyethylene Glycol Additive on the Structure and Performance of Fabric-Reinforced Thin Film Composite". *Molecules*, 2023, 28, 2318.
- [15] Wang, Y., Wang, Z., Lu, W., and Hu, Y., "Review on chitosan-based antibacterial hydrogels: Preparation, mechanisms, and applications". *Int. J. Biol. Macromol.*, 2024, 255, 128080.
- [16] Al-Tayyar, N. A., Youssef, A. M., and Al-Hindi, R. R., "Antimicrobial packaging efficiency of ZnO-SiO₂ nanocomposites infused into PVA/CS film for enhancing the shelf life of food products". *Food Packag. Shelf Life*, 2020, 25, 100523.
- [17] Zhang, X., Li, G., Chen, C., Fan, H., Fang, J., Wu, X., Qi, J., and Li, H., "Chitosan/PVA composite film enhanced by ZnO/lignin with high-strength and antibacterial properties for food packaging". *Int. J. Biol. Macromol.*, 2025, 306, 141658.
- [18] Long, W., Lin, Y., Lv, C., Dong, J., Lv, M., and Lou, X., "High-compatibility properties of Aronia melanocarpa extracts cross-linked chitosan/polyvinyl alcohol composite film for intelligent food packaging". *Int. J. Biol. Macromol.*, 2024, 270, 132305.
- [19] Ju, S., Zhang, F., Duan, J., and Jiang, J., "Characterization of bacterial cellulose composite films incorporated with bulk chitosan and chitosan nanoparticles: A comparative study". *Carbohydr. Polym.*, 2020, 237, 116167.
- [20] Gavriel, B., Bergman, G., Turgeman, M., Nimkar, A., Elias, Y., Levi, M. D., Sharon, D., Shpigel, N., and Aurbach, D. J. M. T. E., "Aqueous proton batteries based on acetic acid solutions: Mechanistic insights". *Mater. Today Energy*, 2023, 31, 101189.
- [21] Guzman-Puyol, S., Benítez, J. J., and Heredia-Guerrero, J. A., "Transparency of polymeric food packaging materials". *Food*

- Res. Int., 2022, 161, 111792.
- [22] Azevedo, A. G., Barros, C., Miranda, S., Machado, A. V., Castro, O., Silva, B., Saraiva, M., Silva, A. S., Pastrana, L., Carneiro, O. S., and Cerqueira, M. A., "Active Flexible Films for Food Packaging: A Review". *Polymers*, 2022, 14, 2442.
- [23] Wardhono, E. Y., Pinem, M. P., Susilo, S., Siom, B. J., Sudrajad, A., Pramono, A., Meliana, Y., and Guénin, E., "Modification of Physio-Mechanical Properties of Chitosan-Based Films via Physical Treatment Approach". *Polymers*, 2022, 14, 5216.
- [24] Murugan, G., Khan, A., Nilsuwan, K., Kim, J. T., Benjakul, S., and Rhim, J.-W., "Chitosan/Polyvinyl Alcohol Based Blend Film Containing Tangerine Peel Carbon Dots: Properties, Antioxidant and Antibacterial Activities". *Waste Biomass Valorization*, 2025, 16, 2255-2270.
- [25] Fakraoui, O., Atanase, L. I., Salhi, S., Royaud, I., Arous, M., and Ayadi, Z., "Investigation of lemon peel extract as a natural additive in polyvinyl alcohol/chitosan blend for advanced bioactive food packaging". *J. Polym. Sci.*, 2024, 1.
- [26] Shokrollahi, M., Bahrami, S. H., Nazarpak, M. H., and Solouk, A., "Multilayer nanofibrous patch comprising chamomile loaded carboxyethyl chitosan/poly(vinyl alcohol) and polycaprolactone as a potential wound dressing". *Int. J. Biol. Macromol.*, 2020, 147, 547-559.
- [27] Narasagoudr, S. S., Hegde, V. G., Vanjeri, V. N., Chougale, R. B., and Masti, S. P., "Ethyl vanillin incorporated chitosan/poly(vinyl alcohol) active films for food packaging applications". *Carbohydr. Polym.*, 2020, 236, 116049.
- [28] Wang, L., Pang, Y., Xin, M., Li, M., Shi, L., and Mao, Y., "Evaluating the antibacterial and antibiofilm activities of chitosan derivatives containing six-membered heterocyclics against *E. coli* and *S. aureus*". *Colloid Surf. B-Biointerfaces*, 2024, 242, 114084.
- [29] Bakhsheshi-Rad, H. R., Ismail, A. F., Aziz, M., Akbari, M., Hadisi, Z., Omid, M., and Chen, X., "Development of the PVA/CS nanofibers containing silk protein sericin as a wound dressing: In vitro and in vivo assessment". *Int. J. Biol. Macromol.*, 2020, 149, 513-521.
- [30] Chamas, A., Moon, H., Zheng, J., Qiu, Y., Tabassum, T., Jang, J. H., Abu-Omar, M., Scott, S. L., and Suh, S., "Degradation Rates of Plastics in the Environment". *ACS Sustain. Chem. Eng.*, 2020, 8, 3494-3511.
- [31] Taktak, F. F. and Kaya, H. N., "Biodegradable PVA/chitosan-based films enriched with rose hip extract and seed oil: Investigation of the influence of tragacanth gum ratio on functional properties and its application in cherry preservation". *Int. J. Biol. Macromol.*, 2025, 307, 141023.
- [32] Yu, Z., Li, B., Chu, J., and Zhang, P., "Silica in situ enhanced PVA/chitosan biodegradable films for food packages". *Carbohydr. Polym.*, 2018, 184, 214-220.
- [33] Ahmed, H., Noyon, M. A. R., Uddin, M. E., Rafid, M. M., Hosen, M. S., and Layek, R. K., "Development and characterization of chitosan-based antimicrobial films: A sustainable alternative to plastic packaging". *Cleaner Chem. Eng.*, 2025, 11, 100157.
- [34] Lal, S., Kumar, V., and Arora, S., "Eco-friendly synthesis of biodegradable and high strength ternary blend films of PVA/starch/pectin: Mechanical, thermal and biodegradation studies". *Polym. Polym. Compos.*, 2020, 29, 1505-1514.
- [35] Yang, H., Wang, L., Xu, C., Hao, W., Xing, R., Liu, S., Yu, H., and Li, P., "Screening for *Aspergillus fumigatus* strain-2T-2 with high chitosanase production activity and its application in chitosan degradation". *Electron. J. Biotechnol.*, 2024, 68, 57-66.